

Proceedings of the International Conference on Oxide Materials for Electronic Engineering, May 29–June 2, 2017, Lviv

Structure and Transport Characteristics of Tunnel Junctions with Hybrid Semiconductor Barriers with Quantum Dots

V.E. SHATERNIK^a, A.P. SHAPOVALOV^{b,*}, T.A. PRIKHNA^b, O.YU. SUVOROV^a, M.A. SKORIK^a,
A.V. SHATERNIK^b, V.I. BONDARCHUK^a AND E.E. ZUBOV^{a,c}

^aG.V. Kurdyumov Institute for Metal Physics, Kyiv 03142, Ukraine

^bV. Bakul Institute for Superhard Materials, Kyiv 07074, Ukraine

^cVasyl' Stus Donetsk National University, Vinnytsia 21021, Ukraine

We propose to realize MoRe/SiO_x(W)/MoRe hybrid junctions by using self-organization effects for the creation of quantum dots (tungsten clusters) in the semiconductor barriers consisting of a mixture of silicon and silicon oxide. Current–voltage characteristics of the MoRe/SiO_x(W)/MoRe samples have been measured in a wide voltage range from –900 to 900 mV at temperatures from 4.2 to 77 K. At low temperatures and for a comparatively small W content in the hybrid barrier, the heterostructures exhibited current–voltage curves of an unusual shape. Single or several current peaks caused by electron tunneling through the allowed states in the barrier have been observed in the transport characteristics. With increasing temperature, superconducting fluctuations in the MoRe electrodes become unimportant, and the current–voltage curve of a heterostructure follows the Ohm law. At last, we present theoretical description of the charge transport in such inhomogeneous systems with account of many-electron processes.

DOI: [10.12693/APhysPolA.133.1060](https://doi.org/10.12693/APhysPolA.133.1060)

PACS/topics: 74.50.+r, 74.81.–g

1. Introduction

Along with the development of semiconductor electronics, significant breakthrough in superconductor electronics can be expected with the development of technologies that allow fabrication of superconducting heterostructures with a precise control on the formation of one-dimensional channels and the transport through quantum dots. The key issue to realize materials with high superconducting characteristics is a related nanoscale design [1, 2]. Synthesis of hybrid (metal clusters in a dielectric matrix) inhomogeneous barriers in superconducting heterostructures represents a convenient tool for creating internal-shunting Josephson junctions [3]. The use of heterostructures with barriers of lower transparency (with a decreased content of a metallic component) [4, 5] made it possible to observe resonant phenomena features in the one-dimensional transport through quantum dots.

The aim of the paper is to study experimentally and theoretically charge transport characteristics of MoRe-based superconducting heterostructures with a hybrid inhomogeneous SiO_x(W) barrier. Our preliminary experimental results were presented at the 2016 Applied Superconductivity Conference (4–9 September, 2016, Denver USA) and published in the materials of the conference [5]. Below we discuss new experimental data together with the previous ones and present an original theoretical approach able to explain related experimental results in the normal state.

2. Fabrication of MoRe/SiO_x(W)/MoRe hybrid structures

MoRe/SiO_x(W)/MoRe (superconductor-barrier-superconductor) structures on Al₂O₃ substrates were fabricated by a magnetron technique. MoRe and SiO_x(W) layers of 100 nm and 15 nm thickness were deposited sequentially with shadow masks by using MoRe-alloy and composite (Si and W) targets. In Fig. 1 a schematic view of the discussed structure is shown. Other deposition details can be found in Ref. [6].

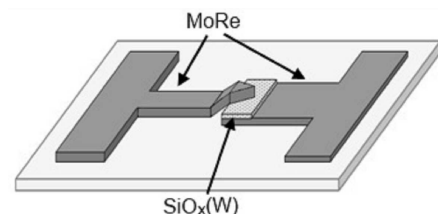


Fig. 1. Geometry of a deposited MoRe/SiO_x(W)/MoRe heterostructure.

To study the structural features, we developed specially designed structures with an increased thickness. The presence and characteristics of tungsten clusters in silicon oxide-based SiO_x(W) films were revealed with a transmission electron microscope (TEM) JEM-2000FX. For the comparison, we fabricated model SiO_x(W) layers of a thickness about 200 nm and studied them with the TEM at accelerating voltage of 200 kV. The obtained results are shown in Fig. 2. It was found that tungsten clusters with diameters of 30–100 nm are formed inside the silicon-oxide layer. Using SiO_x(W) film diffraction patterns (see Fig. 2b and c), we can conclude that both

*corresponding author; e-mail: shapovalovap@gmail.com

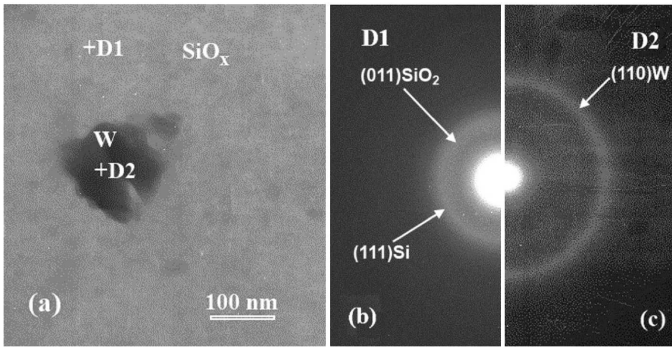


Fig. 2. TEM image of a 200 nm-thick $\text{SiO}_x(\text{W})$ film (a); diffraction patterns of the SiO_x film (b) and a W cluster inside it (c).

silicon-oxide and tungsten layers are amorphous. Indeed, only characteristic halos are seen in the diffraction patterns in Fig. 2, that points to an amorphous state of the material. The broadening of the pattern (see Fig. 2b) can be explained by superposition of two rings which correspond to interplanar spacing for the close-packed planes (111) and (011) in Si and SiO_2 phases, respectively. The film chemical compositions were studied by energy-dispersive analysis using the microscope MIRA 3 TESCAN. They confirmed significant oxygen content in the films, so that the final barrier composition has been close to $\text{Si}_{0.68}\text{O}_{0.32}$. Such high oxygen content is associated with high oxygen activity during the magnetron deposition. It can be substantially reduced only by applying ultrahigh-vacuum evacuation and extremely pure initial mixtures. In our case, the presence of oxygen in the silicon matrix was useful, since it increased the barrier electrical resistance.

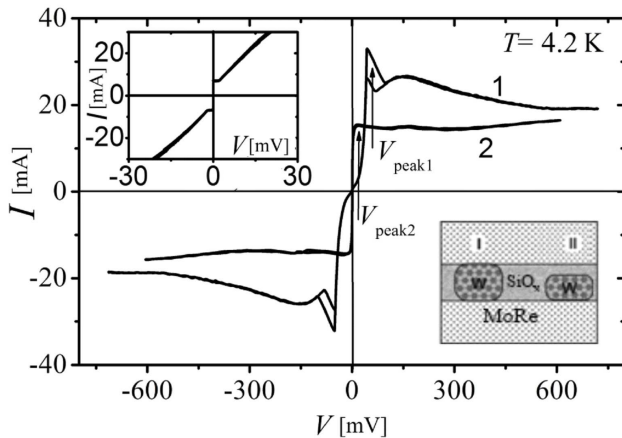


Fig. 3. Current-voltage characteristics of $\text{MoRe}/\text{SiO}_x(\text{W})/\text{MoRe}$ samples at various W contents in a silicon-oxide barrier with the thickness $d = 15$ nm: 1 — $n_W \approx 4$ at.%; 2 — $n_W \approx 5-6$ at.%; the left inset corresponds to $n_W \approx 8$ at.% (this sample showed superconducting current); in the right inset one can see a sketch of the investigated $\text{MoRe}/\text{SiO}_x(\text{W})/\text{MoRe}$ heterostructure with an inhomogeneous hybrid barrier.

In order to develop an adequate model for the transport characteristics of our heterostructures, we have supposed the presence of tungsten nanodots in the dielectric matrix of silicon oxide, see the right inset in Fig. 3. We assume [5] that depending on the content of tungsten in the barrier, the realization of various types of metallic inclusions is possible (see types I and II in the inset of Fig. 3)

3. Current-voltage characteristics of $\text{MoRe}/\text{SiO}_x(\text{W})/\text{MoRe}$ hybrid structures

Current-voltage characteristics (CVCs) of the $\text{MoRe}/\text{SiO}_x(\text{W})/\text{MoRe}$ samples have been measured in a wide voltage range from -900 to 900 mV at temperatures from 4.2 to 77 K. When the W content in a SiO_x barrier was close to $n_W \approx 4$ at.%, we have observed voltage-symmetric resonant current peaks in related CVCs at bias voltages from 40 to 300 mV (e.g., see Fig. 3, curve 1). This type of resonant current peaks in the $I-V$ characteristic of similar heterostructures was demonstrated by us in [5]. When the W content was increased up to $n_W \approx 5-6$ at.%, the bias voltage corresponding to the resonant current peak V_{peak} decreased to several millivolts, and the current peak became wider (see Fig. 3, curves 2). Besides, one can see a negative differential resistance region in the CVCs (see Fig. 3, curves 1 and 2). When the W content in the SiO_x barrier increased up to $n_W \approx 8$ at.%, like in [5] we have observed a superconducting current generated by the Andreev reflections at the MoRe/SiO_x interfaces and the charge flow through the Andreev bound states.

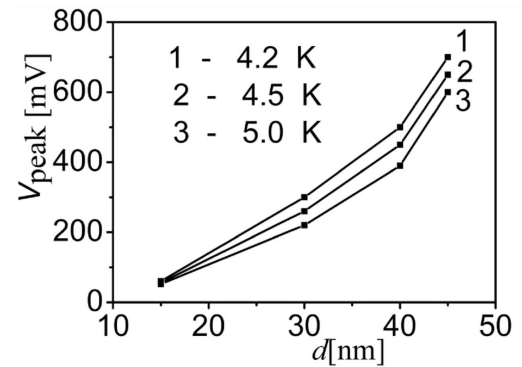


Fig. 4. The peak position V_{peak} , see Fig. 3, as a function of the hybrid barrier thickness d , $n_W \approx 4$ at.%.

The experimentally measured current peak positions V_{peak} (along the bias voltage axis) in the $I-V$ characteristic of the investigated heterostructures as a function of the thickness of the hybrid barrier d are shown in Fig. 4 at various temperatures T . It can be seen that the dependence of $V_{peak}(d)$ is essentially nonlinear, and the value of V_{peak} increases rapidly with the hybrid barrier Si(W) thickness. Nevertheless, the presence of the resonance current peak in the current-voltage characteristic is seen up to a thickness of 45 nm and demonstrates a high transparency of the investigated barrier. It is known [7] that

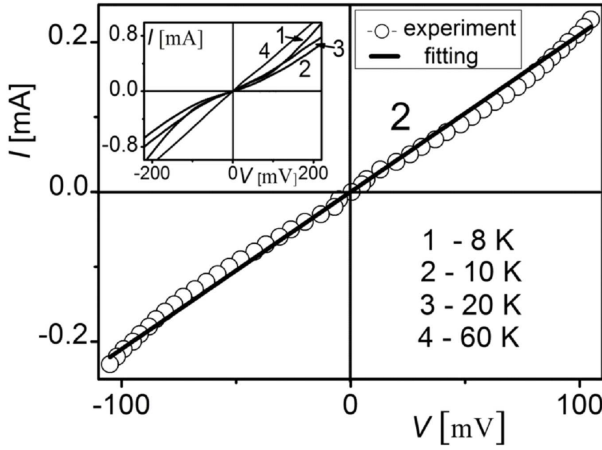


Fig. 5. Theoretical current-voltage curve (solid line) calculated within the framework of the proposed theoretical approach is combined with the experimental one (curve 2, shown by open circles) measured at $T = 10$ K for a heterostructure MoRe/SiO_x(W) barrier/MoRe with the W content close to $n_W \approx 4$ at.%, $d = 15$ nm. The inset shows the same characteristics at various temperatures.

an amorphous silicon contains a large number of shallow traps for electrons. Electrons trapped into them form charge layers that act as potential barriers. It can explain the fact that the position of the observed peak depends on the thickness of the barrier layer.

In the inset in Fig. 5 we demonstrate CVCs of MoRe/SiO_x(W)/MoRe heterostructures at various temperatures for the W content in the SiO_x(W) barrier close to $n_W \approx 4$ at.% and for the barrier thickness ≈ 15 nm. One can see that the resonant-current peaks discussed above disappear at temperatures T above the critical superconducting temperature $T_{c\text{MoRe}} \approx 8.5$ K of the MoRe thin films, and at $T > 10$ K the CVCs are already linear, since the effect of superconducting fluctuations in the MoRe electrodes is low. It means that the current peaks are caused by matching a state localized in a W cluster within the barrier with an edge of the superconducting energy gap in the MoRe electrode. Thus, the peaks are strongly enhanced by the well-known BCS singularity in the density of quasiparticle states of superconductor near the gap energy.

The main transport characteristics of our samples clearly exhibit the presence of high-transparent channels within the barriers. It means that the conventional tunneling theory for extremely rare transferring events should be reconsidered in order to reproduce the observed CVC features. We have realized it by generalizing the Kubo theory using the time-ordering product of perturbation operators. The new theoretical approach to the tunneling problem with account of next orders in the expansion of the current in powers of the tunneling probability $|T|^2$ is presented in the next section.

4. Many-electron processes in charge transport across potential barriers: a new approach

Below we discuss the electron transport through a hybrid structure left (L) normal metal-tunnel barrier-right (R) normal metal [8]. The Hamiltonian of the problem reads as $\hat{H} = \hat{H}_0 + \hat{H}_T$, where $\hat{H}_0 = \hat{H}_L + \hat{H}_R$,

$$\hat{H}_L = \sum_p (\varepsilon_k - \mu_L) n_k = \sum_p \xi_k n_k,$$

$$\hat{H}_R = \sum_p (\varepsilon_p - \mu_R) n_p = \sum_p \xi_p n_p.$$

ε_k and ε_p are electron energies and $n_k = a_k^+ a_k$ and $n_p = a_p^+ a_p$ are particle number operators, μ_L and μ_R are chemical potentials in the L and R electrodes, respectively. The applied voltage V shifts the chemical potentials relatively one another $\mu_L - \mu_R = eV$, where e is absolute value of the electron charge. The perturbation Hamiltonian \hat{H}_T describes electron tunneling processes from the left part of the hybrid structure to the right one [8] $\hat{H}_T = \sum_{kp} (T_{kp} a_k^+ a_p + T_{kp}^* a_p^+ a_k)$. The mean current equals to

$$\langle I \rangle = \sum_{j=0}^{\infty} (-i)^k \int_{-\infty}^t dt_j dt_{j-1} \dots dt_1 \times \left\langle T_t \left\{ I(t) \tilde{A}(t_1) \tilde{A}(t_2) \dots \tilde{A}(t_j) \rho_0 \right\} \right\rangle_{0 \text{ con}},$$

where $\tilde{A}(t_j) = \sum_{kp} \{ \tilde{T}_{1kp} e^{ieVt_j} a_k^+(t_j) a_p(t_j) + \tilde{T}_{2kp} e^{-ieVt_j} a_p^+(t_j) a_k(t_j) \}$, $\tilde{T}_{1kp} = (f(\xi_p) - f(\xi_k)) T_{kp}$, $\tilde{T}_{2kp} = -\tilde{T}_{1kp}^*$, ρ_0 is the unperturbed density matrix, the operators are in the interaction representation and the symbol $\langle T_t \{ \dots \} \rangle_{0 \text{ con}}$ designates a mean on all linked diagrams.

The current expression in the linear approximation takes the form

$$\langle I \rangle_1 = 2e \sum_{kp k_1 p_1} \int_{-\infty}^t dt_1 \times \left\langle T_t \left\{ \left[e^{ieVt} T_{kp} a_k^+(t) a_p(t) - e^{-ieVt} T_{kp}^* a_p^+(t) a_k(t) \right] \times \left[\tilde{T}_{1k_1 p_1} e^{ieVt_1} a_{k_1}^+(t_1) a_{p_1}(t_1) + \tilde{T}_{2k_1 p_1} e^{-ieVt_1} a_{p_1}^+(t_1) a_{k_1}(t_1) \right] \tilde{\rho}_0 \right\} \right\rangle_{0 \text{ con}}. \quad (1)$$

The integral over t_1 in Eq. (4) is calculated without any problems. To take the sum over wave vectors we assume constant electron densities D_L and D_R as well as $|T_{kp}|^2 = |T|^2$. Then at the temperature $T = 0$ the Fermi functions may be replaced by step functions and as a result we get [8]:

$$\langle I \rangle_1 = \frac{4\pi e}{\hbar} |T|^2 D_L D_R \times \int_{-E_F}^{+\infty} d\xi_R [\theta(-(\xi_R - eV)) - \theta(-\xi_R)] =$$

$$\frac{4\pi e}{\hbar} |T|^2 D_L D_R \int_0^{eV} d\xi_R = \frac{4\pi e^2}{\hbar} |T|^2 D_L D_R V$$

i.e., the Ohm law [9].

In the third order of the tunneling probability magnitude it follows that

$$\langle I \rangle_3 = -i \int_{-\infty}^t dt_1 dt_2 dt_3 \times \left\langle T_t \left\{ I(t) \tilde{A}(t_1) \tilde{A}(t_2) \tilde{A}(t_3) \tilde{\rho}_0 \right\} \right\rangle_0 \text{con.} \quad (2)$$

Following (5) it is obtained for $\langle I \rangle_3$:

$$\langle I \rangle_3 = \frac{8\pi^3 e}{\hbar} |T|^4 D_L^2 D_R^2 \int_{-E_F}^{+\infty} d\xi_R [f(\xi_R - eV) - f(\xi_R)]^3 = \frac{8\pi^3 e^2}{\hbar} |T|^4 D_L^2 D_R^2 \int_0^{eV} d\xi_R = \frac{8\pi^3 e^2}{\hbar} |T|^4 D_L^2 D_R^2 V.$$

Summing up the contributions for all orders we obtain a geometric series for $2\pi^2 |T|^2 D_L D_R < 1$. The general expression for the current $\langle I \rangle$ at $T = 0$ has the form of the well-known Landauer formula [10] with a renormalized barrier transparency $\tilde{T} = 2\pi^2 |T|^2 D_L D_R$:

$$\langle I \rangle = \frac{4\pi e^2}{\hbar} \frac{|T|^2 D_L D_R}{1 - 2\pi^2 |T|^2 D_L D_R} V = \frac{2e^2}{\hbar} \frac{2\tilde{T}}{1 - \tilde{T}} V. \quad (3)$$

From Eq. (3) it follows that at $\tilde{T} = 1$ the conductance goes to infinity since the scattering centers are absent. Only at $\tilde{T} = 1/3$ we get a ballistic transport with the Landauer conductivity $G = 2e^2/h$. The latter conclusion can be important also for the further improvement of the so-called tunneling model of the proximity effect [11] where the excitation spectrum of an inhomogeneous superconducting sample is described by transferring electrons between normal and superconducting regions, and the improvement of this theoretical model is also useful for analyzing the behavior of superconducting tunnel junctions with the proximity effect, promising for practical applications [12]. In this case, the measured density of states essentially differs from the conventional one in the BCS theory [13].

Returning to our junctions, we have used the experimental data for a normal-state MoRe 15 nm thick $\text{SiO}_x(\text{W})$ barrier-MoRe trilayer with a small content of tungsten in order to calculate the barrier transparency. From linear fitting to the measured CVC (see curve 2 in Fig. 5) with Eq. (6) we have obtained the effective transparency $\tilde{T} = 0.963$. A small deviation of the $I-V$ curve from the linear dependence near $V = 0$ possibly reflects the presence of superconducting fluctuations at temperatures slightly above T_c .

5. Conclusions

Our structural studies of MoRe/ $\text{SiO}_x(\text{W})$ /MoRe heterostructures fabricated using self-organization effects

have shown the presence of nanoscale metallic inclusions within the silicon-oxide interlayer. We have applied this observation to interpret the effects of the W content and temperature on the shape of the $I-V$ curves which are known to be strongly nonlinear for tunneling across barriers with metallic dots [14]. To explain the charge transport across the inhomogeneous interlayer, we have developed a new theoretical approach which is not limited by a conventional tunneling approximation of ultra-low barrier transparency but rather takes into account many-electron processes. We have found that in our samples the effective transparency of the $\text{SiO}_x(\text{W})$ interlayer was equal to 0.963, that indicates the resonance character of the charge current through the barrier. The modification of the conventional tunneling theory can be useful not only for the junction problem but also for further improvement of the proximity effect theory [11] and explanation of unusual phenomena in superconducting metal oxides [15, 16].

Acknowledgments

V.E.S., A.P.S. and O.Yu.S. were supported by a joint Ukrainian-French grant from the MES of Ukraine. The work by E.E.Z. was carried out within the Fundamental Research Programme funded by the MES of Ukraine (Project No. 0117U002360).

References

- [1] T.A. Prikhna, W. Gawalek, Ya.M. Savchuk, V.M. Tkach, N.I. Danilenko, M. Wendt, J. Delith, H. Weber, M. Eisterer, V.E. Moshchil, N.V. Sergienko, A.V. Kozyrev, P.A. Nagorny, A.P. Shapovalov, V.S. Melnikov, S.N. Dub, D. Litzkendorf, T. Habisreuther, Ch. Schmidt, A. Marmalis, V. Sokolovsky, V.B. Sverdun, F. Karau, A. Starostina, *Physica C* **470**, 935 (2010).
- [2] T.A. Prikhna, W. Gawalek, Ya.M. Savchuk, N.V. Sergienko, V.E. Moshchil, V. Sokolovsky, J. Vajda, V.N. Tkach, F. Karau, H. Weber, M. Eisterer, A. Joulain, J. Rabier, X. Chaud, M. Wendt, J. Delith, N.I. Danilenko, T. Habisreuther, S.N. Dub, V. Meerovich, D. Litzkendorf, P.A. Nagorny, L.K. Kovalev, Ch. Schmidt, V.S. Melnikov, A.P. Shapovalov, A.V. Kozyrev, V.B. Sverdun, J. Kosa, A.V. Vlasenko, *Acta Phys. Pol. A* **117**, 7 (2010).
- [3] V. Lacquaniti, C. Cassiago, N. De Leo, M. Fretto, A. Sosso, P. Febvre, V. Shaternik, A. Shapovalov, O. Suvorov, M. Belogolovskii, P. Seidel, *IEEE Trans. Appl. Supercond.* **26**, 1100505-1 (2016).
- [4] V.E. Shaternik, A.P. Shapovalov, A.Y. Suvorov, N.A. Skoryk, M.A. Belogolovskii, *Low Temp. Phys.* **42**, 426 (2016).
- [5] V.E. Shaternik, A.P. Shapovalov, T.A. Prikhna, O.Yu. Suvorov, M.A. Skorik, V.I. Bondarchuk, V.E. Moshchil, *IEEE Trans. Appl. Supercond.* **27**, 1800507 (2017).
- [6] V. Shaternik, A. Shapovalov, M. Belogolovskii, A. Suvorov, S. Döring, S. Schmidt, P. Seidel, *Mater. Res. Exp.* **1**, 026001 (2014).

- [7] H. Fritzsche, *Amorphous Silicon and Related Materials*, World Sci., Chicago 1989.
- [8] E.E. Zubov, *Phil. Mag.* **98**, 329 (2018).
- [9] G.D. Mahan, *Many-Particle Physics*, 3rd ed., Springer, New York 2000.
- [10] R. Landauer, *Philos. Mag.* **21**, 863 (1970).
- [11] W.L. McMillan, *Phys. Rev.* **175**, 537 (1968).
- [12] V.M. Pan, V.P. Gorishnyak, E.M. Rudenko, V.E. Shaternik, M.V. Belous, S.A. Koziychuk, F.I. Korzhinsky, *Cryogenics* **23**, 258 (1983).
- [13] M.I. Tsindlekht, V.M. Genkin, G.I. Leviev, I. Felner, O. Yuli, I. Asulin, O. Millo, M.A. Belogolovskii, N.Yu. Shitsevalova, *Phys. Rev. B* **78**, 024522 (2008).
- [14] M.A. Belogolovskii, *Cent. Eur. J. Phys.* **7**, 304 (2009).
- [15] V.M. Svistunov, M.A. Belogolovskii, A.I. Khachaturov, *Usp. Fiz. Nauk* **163**, 61 (1993).
- [16] R. Comin, A. Damascelli, *Annu. Rev. Condens. Matter Phys.* **7**, 369 (2016).